Electromechanical actuators affected by multiple failures: a simulated-annealing-based fault identification algorithm

Electromechanical actuators affected by multiple failures: a simulated-annealing-based fault identification algorithm

M. D. L. Dalla Vedova, D. Lauria, P. Maggiore, and L. Pace

***Abstract* —** The identification of early evidences on monitored parameters allows preventing incoming faults. Early alerts can avoid rate of the failures and trigger proper out-of-schedule maintenance activities. For this purpose, there are many prognostic approaches. This paper takes into account a primary flight command electromechanical actuator (EMA) with multiple failures originating from progressive wear and proposes a fault detection approach that identifies symptoms of EMA degradation through a simulated annealing (SA) optimization algorithm; in particular, the present work analyses the functioning of this prognostic tool in three different fault configurations and it focuses on the consequences of multiple failures. For this purpose, we developed a test bench and obtained experimental data necessary to validate the results originated from the model. Such comparison demonstrates that this method is affordable and able to detect failures before they occur, thus reducing the occurrence of false alarms or unexpected failures.

***Keywords*—**Electromechanical actuator, multiple fault detection and evaluation, numerical modeling, prognostics.

I. Introduction

ACTUATORS are devices conceived to convert power from various sources (mechanical, electrical, hydraulic, or pneumatic) into motion. Such conversion is commonly used on aircraft systems to operate flight control surfaces and several utility systems. Reliability of the primary flight controls plays a key role for the safety of the aircraft system and are designed with a conservative safe-life approach which imposes to replace the related components subsequently to a certain number of flight hours (or operating cycles); they are required to be highly reliable (e.g. to exhibit less than one catastrophic failure per 105 flight hours for F-18 and one per $18x10^6$ flight hours for F-35AB [1]).

D. Lauria is with the Department of Mechanical and Aerospace Engineering (DIMEAS), Politecnico di Torino, Corso Duca degli Abruzzi, 24 - 10129 - Torino, ITALY. (e-mail: davide.lauria@yahoo.it).

P. Maggiore is with the Department of Mechanical and Aerospace Engineering (DIMEAS), Politecnico di Torino, Corso Duca degli Abruzzi, 24 - 10129 - Torino, ITALY. (e-mail: paolo.maggiore@polito.it).

L. Pace is with the Department of Mechanical and Aerospace Engineering (DIMEAS), Politecnico di Torino, Corso Duca degli Abruzzi, 24 - 10129 - Torino, ITALY. (e-mail: lorenzo.pace@polito.it).

M. D. L. Dalla Vedova is with the Department of Mechanical and Aerospace Engineering (DIMEAS), Politecnico di Torino, Corso Duca degli Abruzzi, 24 - 10129 - Torino, ITALY. (corresponding author phone: +390110906850; e-mail: matteo.dallavedova@polito.it).

A defined program of scheduled maintenance should guarantee that the system operates always in safety conditions. Nevertheless, the system could be unexpectedly exposed to extreme operative scenarios, with consequent damage and unscheduled maintenance, increased risk and costs, and possibly impact on mission. The monitoring of functional parameters of the considered system permits to determine if an anomalous behavior is starting to occur at an early stage. This also enables to determine the source of the anomalous behavior. A high level of reliability can guarantee the prediction of this kind of failures. The discipline aimed to do so is called Prognosis and Health Management system (commonly abbreviated with the acronym PHM) [2] or Prognostics; the application of the PHM strategies typically requires monitoring a set of system parameters in the form of electric signals. As a consequence, the application of PHM is favored on electrical systems, where no additional sensor is required, as the same sensors used to the control scheme and system monitors can be used also for PHM [2]. Prognostics are usually applied to mechatronic systems having a complex non-linear multidisciplinary behavior. Literature proposes a wide range of failure detection and identification strategies, among these: (as reviewed in [3]) model-based techniques based on the direct comparison between real and monitoring system [4], on spectral analysis of well-defined system behaviors (typically performed by Fast Fourier Transform FFT) [5], on appropriate combinations of these methods [6] or Artificial Neural Networks [7]. The study presented in this paper considers electro-mechanical actuation systems, which follow the "More-" [8] and the "All-electric-aircraft" [9] paradigms. It must be noted that the concepts and the results reported in this paper are part of a wider research activity focused on the diagnosis model-based approach and, in particular, on the parametric estimation task. The main goal of the research is the design of a modern and fast damage estimator routine for a simple (but real) electromechanical actuation system, in order to prove its accuracy and reliability. In [3] is described a similar approach that aims to obtain a prediction of faults linked to increased friction torque. To this purpose, authors realized and modeled a test-bench electromechanical actuator (EMA) to compare its real behavior with the predicted values at the aim to optimize and validate a prognostic algorithm based on the simulated annealing method [10].

II. Aims of Work

This paper is aimed to extend the prognostic application of the simulated annealing approach proposed in [3] to a system with combined progressive faults. Different combinations of the considered faults (seizure and backlash) have been examined to evaluate the accuracy of the predictions at the different conditions and to assess the field of validity of the proposed prognostic method.

In particular, three faults combinations cases have been considered:

1) moderate seizure and low backlash,
2) low seizure and high backlash,
3) very low seizure and very low backlash.

These three cases have been numerically simulated through the modification of the original EMA model.

III. Electromechanical Actuator Model

Primary flight controls are typically proportional servomechanisms with continuous activation: they must return a force feedback related to command intensity and a high frequency response. Their purpose is to control the dynamic of the aircraft by generating, by means of a proper rotation of the corresponding aerodynamic surfaces, unbalanced forces and couples acting on the aircraft itself.

These controls are usually conceived to obtain the aircraft rotation around one of the three body axis when one control surface is activated, possibly minimizing the coupling effects. Until a few years ago, the actuators mainly used in aeronautical applications were generally hydraulic and precisely hydromechanical or, more recently, electrohydraulic.

This kind of actuator, because of its great accuracy, high specific power and very high reliability, is often equipped on current aircrafts, even if on more modern airliners electro-hydrostatic actuators (EHA) or electro-mechanical actuators (EMA) are installed.

As shown in Fig. 1, a typical EMA used in a primary flight control is composed of:

1) an actuator control electronics (ACE) that closes the feedback loop, by comparing the commanded position (FBW) with the actual one, elaborates the corrective actions and generates the reference current Iref;
2) a Power Drive Electronics (PDE) that regulates the three-phase electrical power;
3) an electrical motor, often BLDC (Brush-Less Direct Current) type;
4) a gear reducer having the function to decrease the motor angular speed (RPM) and increase its torque to desired values;
5) a system that transforms rotary motion into linear motion: ball screws or roller screws are usually preferred to acme screws because, having a higher efficiency, they can perform the conversion with lower friction;
6) a network of sensors used to close the feedback rings (current, angular speed and position) that control the whole actuation system.

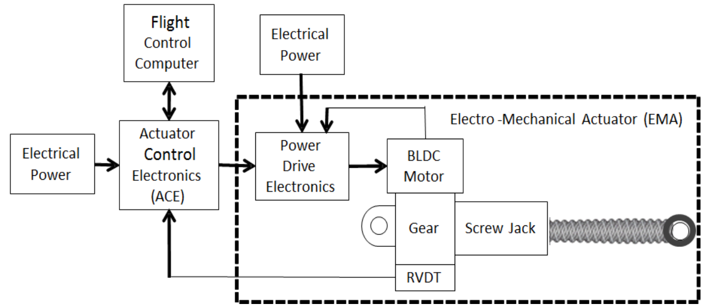

Fig. 1 electromechanical actuator scheme

The proposed numerical model, as reported in [11], is composed of six blocks representing the different physical or functional components of the real onboard EMA (Fig. 1). The corresponding Simulink model (Fig. 2), is composed of the following six functional blocks:

1) PID Control Logic (modelling a Proportional-Integrative-Derivative controller with saturated output and anti-windup device);
2) Controller (simulating the EMA controller behaviors);
3) Motor (simplified electro-magneto-mechanical model of the considered BLDC motor);
4) Gear box;
5) Ball screw;
6) Encoder.

As shown in [7], every block has been modeled starting from its basic electromechanical equations, but since the objective is to achieve a model capable to recognize defined actuator progressive faults (e.g. dry friction or mechanical backlash), it was decided to model in a suitably simplified way the electromagnetic aspects and focus instead on mechanical ones. In particular, the considered numerical model is developed from the monitoring model conceived by the authors for an EMA model-based prognostic application [12].

The electro-magneto-mechanical dynamics of the BLDC motor is simulated by means of a classic resistive-inductive (RL) numerical model. In particular, it is a 1st order linear model capable of calculating the moving torque TM as a function of the motor torque gain GM, of its power supply voltage (*Vdcm·I_ref*), of the counter-electromotive forces (back-emf), of the dynamic characteristics of the RL circuit and of the saturation of magnetic induction flux.

The dynamics of the mechanical actuation system (rotor of BCD motor, gear box and ball screw) is represented by a simplified 1 degree-of-freedom system (obtained assuming an ideal rigid transmission without elastic deformations or backlashes). According to [7], it is modelled by means of a 2nd order non-linear numerical model able to simulate the EMA behavior taking into account the global effects due to inertia, viscous damping, ball screw ends-of-travel and dry frictions. As shown in Fig. 3, the global value of the dry friction torques acting on the actuation system is simulated by a simplified numerical algorithm which implements the classical Coulomb's model.

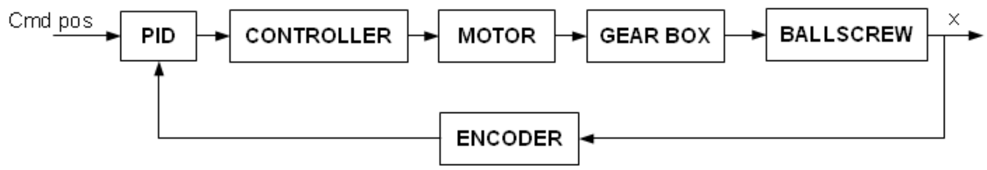

Fig. 2 conceptual model scheme

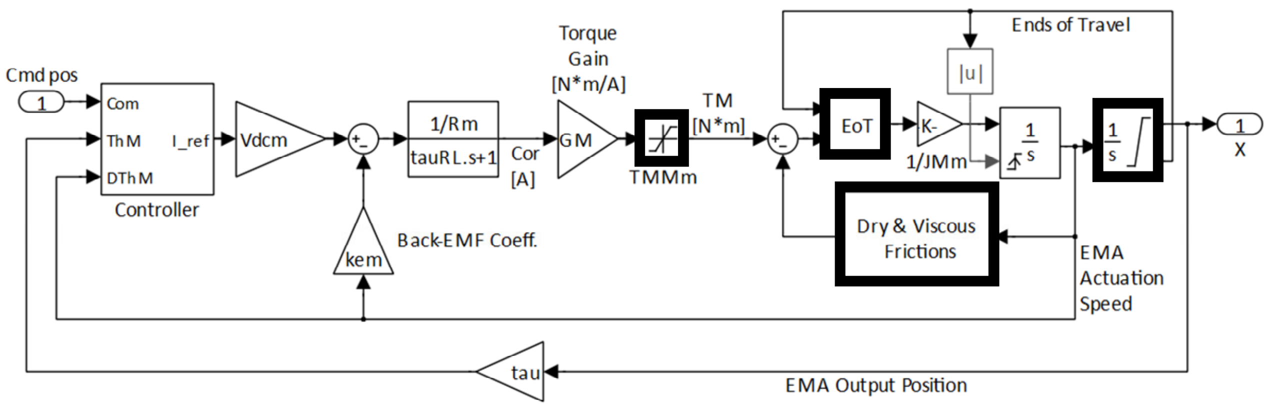

Fig. 3 block Diagram of EMA numerical model: the blocks that implement the nonlinearities considered (saturation of the motor torque, friction phenomena and ends-of-travels acting on the final ballscrew actuator) are highlighted in the diagram by bold border

In particular, the proposed algorithm has been developed by means of a lumped parameter model based on the Karnopp friction model [13] and suitably modified as shown in [14].

The effects of the backlashes affecting the mechanical transmission, evaluated according to [15], have been simulated, using a simplified approach, by the "Backlash" Simulink block [16].

IV. Optimization Algorithm

Several optimization techniques are commonly used also for model parameter estimation tasks, which can be classified into two main categories: deterministic (direct or indirect) and probabilistic (stochastic, as Monte Carlo method, simulated annealing and genetic algorithms). A large part of these methods are local minima search algorithms and often do not find the global solution [5]. They are therefore highly dependent on a good initial setting. This is a viable solution in an off-line scenario, where initial guesses can be reiterated; on the other hand, these approaches are not suitable for an on-line automated identification process, because a good initial guess for one data set may not be such for the next identification. Local-minima approaches would not be robust and may provide a false indication of parameter changes in an on-line system. Alternatively, global search methods, such as genetic algorithms and simulated annealing, provide more promising options for on-line model identification. However, as they are similar to simplex methods, genetic algorithms do not always find the global minima [17]. Simulated annealing methods are more effective at finding the global minima, but at the cost of a larger amount of iterations [2].

The simulated annealing method originates, as the name suggests, from the study of thermal properties of solids. Indeed, this procedure, as described in [18], was then an exact copy of the physical process which could be used to simulate a collection of atoms in thermodynamic equilibrium at a given temperature. In fact, the abstraction of this method in order to allow arbitrary problem spaces is straightforward.

There is a significant correlation between the terminology of thermodynamic annealing process (the behavior of systems with many degrees of freedom in thermal equilibrium at a finite temperature) and combinatorial optimization (finding global minimum of a given function based on many parameters). A detailed analogy of annealing in solids provides frame work for optimization. As described in [19], the Table 1 summarizes the key terms which are related with the real thermodynamic annealing procedure, showing its association with the aforesaid optimization process.

Table 1: Association between thermodynamic simulation and combinatorial optimization

Thermodynamic Annealing	**Combinatorial Optimization**
System State	Feasible Solutions
Energy of a State	Cost of Solution
Change of state	Neighbor solution
Temperature	Control parameter
Minimum Energy	Minimum Cost

In order to explain more clearly the association between thermodynamic simulation and combinatorial optimization reported in Table 1, it should be noted that the **cost of a solution** represents the corresponding objective function value (i.e. the function that the optimization algorithm attempts to minimize in order to identify the optimal solution), the **neighbor solution** is a new system solution calculated by the optimization algorithm and evaluated, with respect to the previous one, using the said cost functions, and the **control parameter** is the system parameter iteratively modified by the optimization process so as to minimize its objective function.

Figure 4 shows the operating logic of the method.

V. Proposed Prognostic Algorithm

The EMA nonlinear numerical model is able to simulate the system response [11], considering both Coulomb friction and backlash, being then potentially able to reproduce seizure due to the ball return jamming or bearing binding/sticking as well as the appearance of backlash in case of balls excessive wear.

As a consequence, its execution speed has been tested in order to verify its suitability for optimization purposes. It must be noted that, despite being a relatively simplified numerical model, it shows a good accuracy, guaranteeing a satisfying correspondence with the experimental data (as reported in the following sections). The method performs the failure detection and identification using an optimization process implemented by a simulated annealing (SA) algorithm that aims to minimize the value of appropriate objective functions (typically related to the magnitude of the error E_{int} calculated comparing together experimental and numerical data) by acting on well-defined parameters of the numerical model.

In particular, by means of a simulated annealing algorithm, the optimization process modifies the parameters CSJ and BKL*,* the former representative of the dry frictions, the latter of the mechanical backlashes globally acting on the EMA numerical model, in order to identify their values that minimize the above mentioned objective functions.

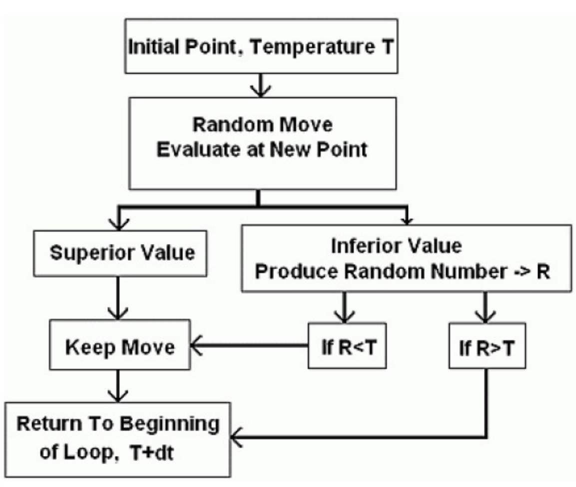

Fig. 4 Operating Logic of Simulated Annealing Method

In this case, the objective function of the optimization problem is the error generated, by a well-defined command input (*Cmd pos*), between the experimental data and the corresponding model output. Before verifying the actual ability of the proposed prognostic method to identify and evaluate failure precursors, the calibration of the numerical model parameters has been performed. As shown in [3], the ideal values of these parameters have been identified by comparing the dynamic response of the real system in nominal conditions (NC: e.g. nominal dry friction and mechanical backlash levels and no other failures) with that generated by the numerical model, then, identifying the corresponding objective function (E_{int}) and, at last, applying the proposed optimization process to the above parameters.

The aforesaid model, properly calibrated in NC, was then used to estimate the global amount of the dry friction and mechanical backlash acting on the real EMA; the dynamic response of the real EMA (subjected to a well-defined system of backlashes affecting the mechanical transmission) is compared with that produced by the simulation model and, by the optimization method, the values of the fault parameters CSJ and BLK[1] that minimize the error between real and simulated is calculated. The SA method used by the proposed prognostic routine to perform the aforesaid fault estimation is implemented by the Matlab Optimization Tool. It must be noted that these optimizations have been carried out in condition of unloaded actuator since, within an operational scenario, these kinds of tests could be performed on the ground, without any aerodynamic loads, but rather just with the control surface weight, which is usually negligible compared to the actuator's capabilities.

The problem of what type of signal should have been used to test the optimization algorithm has not a precise solution and depends strongly by the system's application. In the case here examined, a sinusoidal linear frequency sweep wave has been chosen as a standard input position signal for the parameter estimation process because it allows testing, at one time, a wide range of system response frequencies[2]. For instance, in the low frequency range the stick-slip motion could be highlighted, enabling the optimization algorithm to finely tune the friction and backlash coefficients of the model and, at the same time, adapt the other parameters according also to the high frequency range, representing more significantly the system dynamic response. A simple step or ramp response could not comply with this necessity.

1 The parameter BLK takes into account the global effects of the backlashes affecting the EMA mechanical transmission by means of a very simplified model; in fact, the dynamic interactions between the different elements interested to the above mentioned backlashes are neglected. Dimensionally speaking, BLK is expressed in millimetres and it is representing the equivalent mechanical backlash (that is calculated as a sum of the backlash affecting the components of the transmission) acting on the whole EMA.

2 For instance, in the low frequency range the stick-slip motion could be highlighted, enabling the optimization algorithm to finely tune the friction and backlash coefficients of the model and, at the same time, adapt the other parameters according also to the high frequency range, representing more significantly the system dynamic response.

In order to obtain accurate results and assure a suitable speed of convergence of the algorithm, the variation range of the parameters representative of the considered progressive failures CSJ and BKL (which vary during the optimization process to minimize the error between experimental data and corresponding numerical simulations) have been limited between properly defined lower and upper bounds.

In particular, CSJ can assume values from 0.01 Nm to 1.5 Nm which represent a quite large band given that its initial value is assumed equal to 0.12 Nm (NC dry frictional torque provided by motor datasheet) and the corresponding peak torque provided by the DC motor is worth 1.48 Nm.

In a similar manner, it is also necessary identify some meaningful value regarding the backlash phenomenon: by reading the MecVel ALI-2 maintenance handbook [12], it is possible to gain knowledge of the maximum acceptable backlash value of the ballscrew:

$$\Delta_b \leq 0.3 \cdot p = 1.5\ mm$$

where p is the ballscrew pitch (5 mm). For higher values of Δ_b, the ballscrew should be replaced. Therefore the afore calculated backlash value can be considered as limit value and clearly it is very far from the healthy value related to the actual system. In this case, BLK can assume values from 0 [mm] (LB) to 0.1 [mm] (UB), which represent a quite large band given that the authors' goal is the proposal of a prognostic method (able to perform an early identification of the considered progressive faults) and the actual value of the mechanical backlash (in healthy conditions) is worth about 0.033 [mm]. Hence, in order to test the algorithm's resolution and accuracy, it would be meaningful to increase the latter value by different percentage, considering mechanical transmissions characterized to different fault magnitude (e.g. gears or screw suitably damaged) or modifying the experimental results in order to simulate the backlash effects.

To this purpose, this research evaluates three cases of backlash severity:

1) High: 0.066 [mm];
2) Moderate: 0.0495 [mm];
3) Low: 0.04125 [mm].

VI. Evaluation of the Proposed Method

Several experimental tests have been conducted (with different time-history input and different levels of failure) to test the performance of the proposed method; the results of such tests have then been used as input to the optimization process performing the failure analysis. In particular, in order to evaluate the accuracy of the predictions and its sensitivity to the different fault conditions and to assess the field of validity of the proposed prognostic method, three different combinations of the progressive faults (seizure CSJ and backlash BLK) have been evaluated:

1) moderate seizure and low backlash,
2) low seizure and high backlash,
3) very low backlash and seizure.

A. Moderate Seizure and Low Backlash

The following faulty values have been imposed on the numerical model: static friction coefficient CSJ equal to 0.3 [Nm] (+117.4%) and backlash BLK: 0.04125 [mm] (+25%). These faulty values correspond to double the static friction coefficient and slightly increase the backlash value, in respect to the corresponding healthy values.

After an optimization run, the initial objective function of 0.655 [$mm^2 \cdot s$] was reduced by the 99.936% (i.e. $9.39 \cdot 10^{-5}$ [$mm^2 \cdot s$]). The effects of the optimization process on the dynamic response of the simulated system could be evaluated (e.g. in terms of EMA rod position and actuation speed) comparing the corresponding curves calculated before and after the SA optimization process: respectively, Fig. 5 and Fig. 6 for the position, Fig. 7 and Fig. 8 for the actuation speed.

In this case, the algorithm yielded a quite satisfying result, having found a 115.2% increase for CSJ and a 22.23% increase for the backlash value, as shown in Table 2. Thus, the accuracy for CSJ was of 1%, while for backlash it was 2.21%.

Figure 9 shows the corresponding **diagnostic scalars** (i.e. the histogram representing the results performed by the proposed method for the considered case of multiple faults). The diagnostic scalars compare each other the estimated and the actual values of the considered parameters (in this case the BKL and CSJ) putting in evidence the corresponding errors; these values are expressed as a percentage of the related nominal values (NC).

B. Low Seizure and High Backlash

The opposite situation has been tested as well by imposing in the model the following parameter: CSJ equal to 0.1449 [Nm] (+5%) and backlash equal to 0.066 [mm] (+100%). Compared with the healthy conditions, these faulty values correspond to a slightly increase of the friction coefficient and a double of the backlash amount. After about 1500 iterations (corresponding to around thirty seconds of calculation), the damage estimator reduced the objective function value by the 96.5%, giving the results shown in Table 3. Both the estimated shifts have been found by the algorithm with a rather high accuracy. Figure 10 depicts the related final diagnostic scalars.

C. Very Low Seizure and Backlash

In order to test the algorithm's resolution, a final simulation has been carried out with a 1% increase of both seizure and backlash parameters:

- CSJ: 0.13938 [Nm]
- Backlash: 0.03333 [mm]

In this case, the optimization process, which lasted around thirty seconds (about 1500 iterations), reduced the objective function by the 92.6%. Also in this case, the corresponding results are shown in Table 4. The friction increase has been correctly recognized even though underestimated, while the backlash increase resulted significantly wrong and overestimated. Nevertheless, from a prognosis point of view, a 1% increase might not be meaningful. Figure 11 depicts the related final diagnostic scalars.

Table 2: Shift from healthy parameters in case of combined failure mode (moderate seizure and low backlash)

Parameter	Unit	Start	Final	Shift	Actual shift	Accuracy
CSJ	[Nm]	0.138	0.297	+115.2%	+117.4%	1%
Backlash	[mm]	0.033	0.0403	+22.23%	+25%	2.21%

Table 3: Shift from healthy parameters in case of combined failure mode (low seizure and high backlash)

Parameter	Unit	Start	Final	Shift	Actual shift	Accuracy
CSJ	[Nm]	0.138	0.14771	+7.03%	+5%	1.94%
Backlash	[mm]	0.033	0.06545	+98.33%	+100%	2.21%

Table 4: Shift from healthy parameters in case of combined failure mode (very low seizure and backlash)

Parameter	Unit	Start	Final	Shift	Actual shift	Accuracy
CSJ	[Nm]	0.138	0.13896	+0.69%	+1%	0.3%
Backlash	[mm]	0.033	0.03608	+9.33%	+1%	8.25%

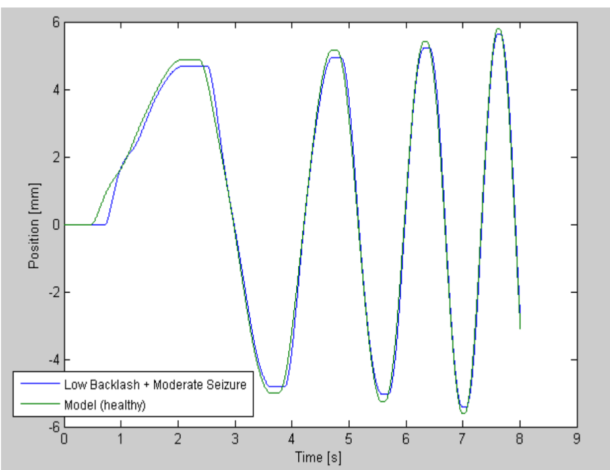

Fig. 5 Moderate seizure and low backlash case: calculated EMA position before SA optimization

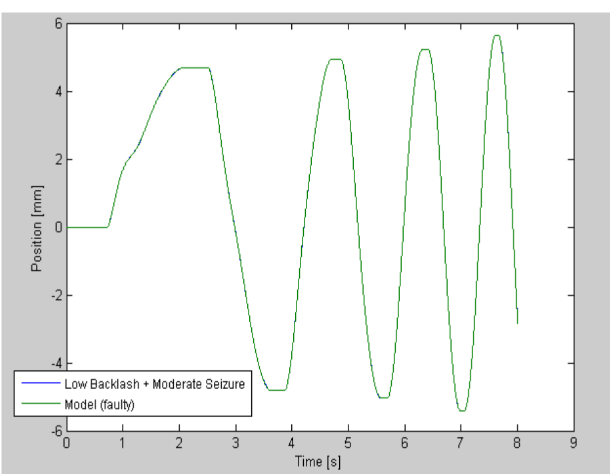

Fig. 6 Moderate seizure and low backlash case: calculated EMA position after SA optimization

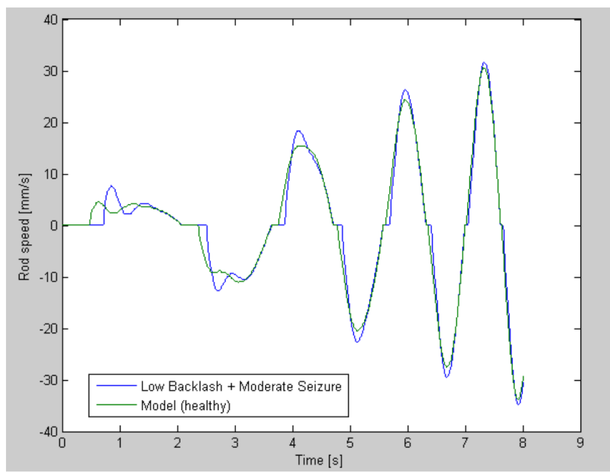

Fig. 7 Moderate seizure and low backlash case: calculated EMA actuation speed before SA optimization

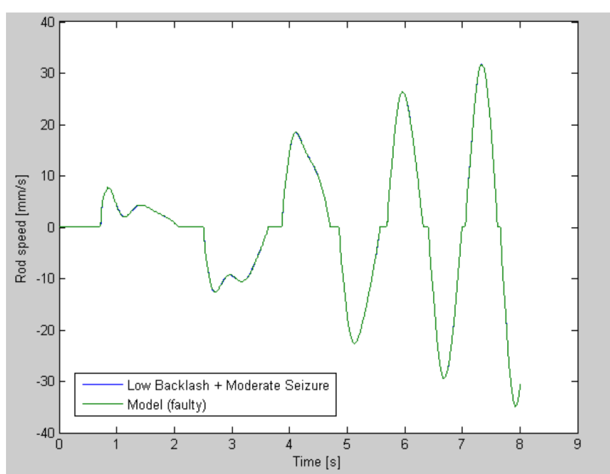

Fig. 8 Moderate seizure and low backlash case: calculated EMA actuation speed after SA optimization

D. Diagnostic Scalars for Multiple Faults

As mentioned earlier, the diagnostic scalars compare each other the estimated and the actual values of the considered parameters (in this case the BKL and CSJ) putting in evidence the errors; these values are expressed as a percentage of the related nominal values (NC). The following figures show all the diagnostic scalars diagram achieved in case of combined failure modes.

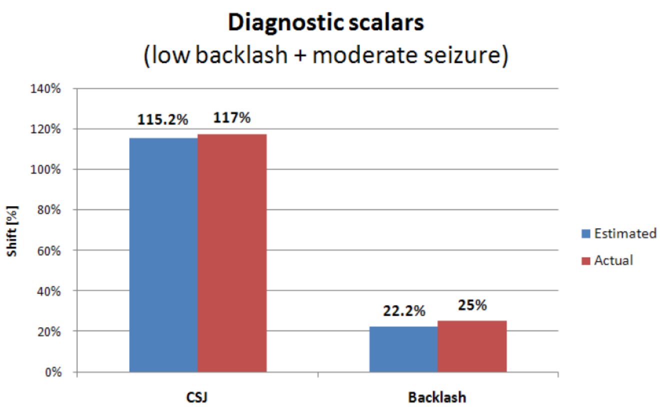

Fig. 9 Diagnostic scalars in case of combined failure modes: moderate seizure and low backlash case

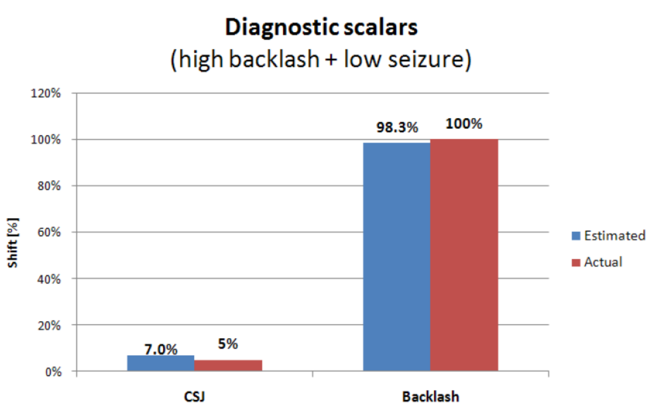

Fig. 10 Diagnostic scalars in case of combined failure modes: low seizure and high backlash case

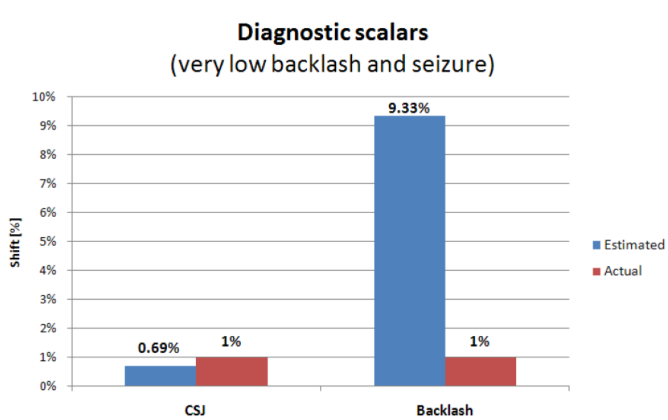

Fig. 11 Diagnostic scalars in case of combined failure modes: very low seizure and backlash case

VII. Conclusions

The method based on the Simulated Annealing algorithm has been used to monitor the sample EMA in different multiple failure modes conditions, and has demonstrated to be able to identify the increase of parameters correctly; however, it failed in the case where a rather low backlash increase percentage was involved. This configuration could represent a limit situation for the algorithm; it is suggested that some minimum shift thresholds are arranged with the aim to avoid false indications on the damage progression. Overall, the results are less accurate when the failure is less severe. Anyway, the algorithm has been able to identify with good approximation a value for CSJ even with very low seizure condition and in general this parameter seems to be described with a better and steadier accuracy than backlash. In fact, the latter resulted to be acceptable mostly for high shift values (e.g. +100%).

The Simulated Annealing proved to be very effective, with fairly acceptable execution times (tenth of minutes) for an operational scenario. However, this method showed a strong dependence of the results on its initialization settings (i.e. initial temperature, function tolerance, reannealing interval) and also on the variables bounds which have to be chosen carefully; this can be achieved making, for example, some considerations regarding the physical limits of initialization settings. Nevertheless, it is noteworthy that no situations caused the algorithm to remain trapped in local minima, even when the starting point was far from the faulty experimental data. This happened, as a comparison, for other deterministic methods like recursive-least-squares, which gave worse results compared to Simulated Annealing. It is possible to conclude that this kind of damage estimator can be considered a good approach for prognostics applications, even for combined failures. Broader use on different study cases is envisaged as fundamental to assess the validity of this method at all the possible different conditions.

Table 5: Summary of the optimization in case of combined failures.

Parameter	Unit	A	B	C
Time	[sec]	75	45	40
Iterations		2535	1651	1500
Object Function		-99.94%	-96.5%	-92.6%
Estimated CSJ	[Nm]	0.297	0.14771	0.13896
Actual CSJ	[Nm]	0.3	0.1449	0.13938
CSJ accuracy		1%	1.94%	0.3%
Estimated CSJ shift		+115.2%	7%	+0.69%
Actual CSJ shift		117%	5%	1%
Estimated backlash	[mm]	0.0403	0.06545	0.03608
Actual backlash	[mm]	0.04125	0.066	0.03333
Backlash accuracy		2.21%	0.83%	8.25%
Estimated backlash shift		+22.2%	+98.3%	+9.33%
Actual backlash shift		25%	100%	1%

ACKNOWLEDGMENT

In conclusion, the authors wish to extend a heartfelt thanks to Professor Lorenzo Borello for his precious role in the definition of the concepts that have allowed the realization of this work and for his essential support.

REFERENCES

[1] DoD Panel to Review the V-22 Program, Report of the Panel to Review the V-22 Program, April 2001.
[2] C. S. Byington, M. Watson, D. Edwards, and P. Stoelting, *A Model-Based Approach to Prognostics and Health Management for Flight Control Actuators*, IEEE Aerospace Conf. Proceedings, USA, 2004.
[3] M. D. L. Dalla Vedova, P. Maggiore, and L. Pace, *A New Prognostic Method Based on Simulated Annealing Algorithm to Deal with the Effects of Dry Friction on Electromechanical Actuators*, International Journal of Mechanics, Vol. 9, 2015, pp. 236-245, ISSN: 1998-4448.
[4] L. Borello, M. D. L. Dalla Vedova, G. Jacazio, and M. Sorli, *A Prognostic Model for Electrohydraulic Servovalves*, Proceedings of the Annual Conf. of the Prognostics and Health Management Society, 2009.
[5] M. D. L. Dalla Vedova, P. Maggiore, and L. Pace. *Proposal of Prognostic Parametric Method Applied to an Electrohydraulic Servomechanism Affected by Multiple Failures*. WSEAS Transactions on Environment and Development, ISSN: 1790-5079, pp. 478-490.
[6] P. Maggiore, M. D. L. Dalla Vedova, L. Pace, and A Desando, *Proposal of fault analysis parametric method applied to an electromechanical servomechanisms affected by failures*, International Journal of Prognostics and Health Management, Vol. 6, 2015, ISSN: 2153-2648.
[7] M. Battipede, M. D. L. Dalla Vedova, P. Maggiore, and S. Romeo, *Model based analysis of precursors of electromechanical servomechanisms failures using an artificial neural network*, Proceedings of the AIAA SciTech Modeling and Simulation Technologies Conference, Kissimmee, Florida, 5-9 January 2015.
[8] R. E. J. Quigley, *More electric aircraft*, Proceedings of Eighth Annual IEEE Applied Power Electronics Conference - APEC '93, San Diego, CA, 7-11 March 1993, pp. 906-911.
[9] M. Howse, *All-electric aircraft*, Power Engineer, Vol. 17, No. 4, 2003, pp. 35-37.
[10] M. F. Cardoso, R. L. Salcedo, and S. F. De Azevedo, *The simplex-simulated annealing approach to continuous nonlinear optimization*, Computers & chemical engineering, Vol. 20, 1996, pp. 1065-1080.
[11] M. D. L. Dalla Vedova, D. Lauria, P. Maggiore, and L. Pace, *Linear Electromechanical Actuators Affected by Mechanical Backlash: a Fault Identification Method Based on Simulated Annealing Algorithm*, WSEAS Transactions On Systems, Vol. 14, 2015, pp. 268-277.
[12] M. D. L. Dalla Vedova, G. Jacazio, P. Maggiore, and M. Sorli, *Identification of precursors of servovalves failures for implementation of an effective prognostics*, International Conference of Recent Advances in Aerospace Actuation Systems and Components, Toulouse (France), 5-7 May, 2010, pp. 116-126, ISBN: 978-2-87649-060-4.
[13] D. Karnopp, *Computer simulation of stick-slip friction in mechanical dynamic systems*, Journal of Dynamic Systems, Measurement, and Control, Vol. 107, No. 1, pp. 100-103, 1985.
[14] L. Borello, and M. D. L. Dalla Vedova, *A dry friction model and robust computational algorithm for reversible or irreversible motion transmission*, International Journal of Mechanics and Control (JoMaC), Vol. 13, No. 02, December 2012, pp. 37-48, ISSN: 1590-8844.
[15] L. Borello, G. Villero, and M. D. L. Dalla Vedova, *New asymmetry monitoring techniques*, Aerospace Science and Technology, Vol. 13, No. 8, December 2009, pp. 475-497.
[16] S. T. Karris, *Introduction to Simulink with Engineering Applications*, Third Edition, Fremont, CA, Orchard Publications, 2011.
[17] M. Pirlot**,** *General Local Search Methods*, European Journal of Operational Research, vol. 92, pp. 493-511, 1996.
[18] N. Metropolis, A. N. Rosenbluth, M. N. Rosenbluth, A. H. Teller, and E. Teller, *Equation of state calculation by fast computing machines***,** Journal of Chemical Physics, Vol. 2, No. 6, pp. 1087-1092, 1953.
[19] K.K. Vishwakarma, H.M. Dubey, M. Pandit, and B.K. Panigrahi, *Simulated annealing approach for solving economic load dispatch problems with valve point loading effects*, International Journal of Engineering, Science and Technology, Vol. 4, No. 4, 2012.

Matteo D. L. Dalla Vedova received the M.Sc. and the Ph.D. from the Politecnico di Torino in 2003 and 2007, respectively. He is currently assistant researcher at the Department of Mechanics and Aerospace Engineering. His research activity is mainly focused on the aeronautical systems engineering and, in particular, is dedicated to design, analysis and numerical simulation of on board systems, study of secondary flight control system and conception of related monitoring strategies and developing of prognostic algorithms for aerospace servomechanism**.**

Davide Lauria received the M.Sc degree in Aerospace Engineering from the Politecnico di Torino in 2010 with a thesis at Cranfield University (UK) on damage estimation by Simulated Annealing for model-based PHM. From 2010 to 2012 he has been quality engineer at APR srl (Italy) and then joined to UTC Aerospace Systems (Italy) as system test rig design engineer unitl 2015. He is currently Gearbox Technical Leader at GE Avio.

Paolo Maggiore is a professor at the Mechanical and Aerospace Engineering Department of Politecnico di Torino, that joined in 1992, where he teaches aerospace general systems engineering. Currently his assistant researchers and PhD students are involved in projects ranging from hydrogen fuel cell powered airplanes and UAVs, and health monitoring of flight controls, to multi-disciplinary design optimization of aerospace systems design.

Lorenzo Pace graduated in Aerospace Engineering at Politecnico di Torino in 2008. Since 2008 to 2011, he worked as an assistant researcher, following studies about system experimental testing and modelization in the aerospace field, with a focus to energy saving techniques. Since 2012 to 2014 he completed a PhD in Aerospace Engineering at Politecnico di Torino, with the contribution of Thales Alenia Space, focused on the application of Model Based System Engineering to verification in the space industry.